

Deep learning adaptive Model Predictive Control of Fed-Batch Cultivations

Niels Krausch^b, Martin Doff-Sotta^a, Mark Cannon^{a,*}, Peter Neubauer^b, Mariano Nicolas Cruz Bournazou^b

^aUniversity of Oxford, Department of Engineering Science, Parks Road, Oxford, OX1 3PJ, UK

^bTechnische Universität Berlin, Institute of Biotechnology, Bioprocess engineering, Ackerstr. 76, Berlin, 13355, Germany

Abstract

Bioprocesses are often characterised by nonlinear and uncertain dynamics, posing particular challenges for model predictive control (MPC) algorithms due to their computational demands when applied to nonlinear systems. Recent advances in optimal control theory have demonstrated that concepts from convex optimisation, tube MPC, and differences of convex functions (DC) enable efficient, robust online process control. Our approach is based on DC decompositions of nonlinear dynamics and successive linearisations around predicted trajectories. By convexity, the linearisation errors have tight bounds and can be treated as bounded disturbances within a robust tube MPC framework. We describe a systematic, data-driven method for computing DC model representations using deep learning neural networks with a special convex structure, and explain how the resulting MPC optimisation can be solved using convex programming. For the problem of maximising product formation in a cultivation with uncertain model parameters, we design a controller that ensures robust constraint satisfaction and allows online estimation of unknown model parameters. Our results indicate that this method is a promising solution for computationally tractable, robust MPC of bioprocesses.

Keywords: Nonlinear model predictive control, robust adaptive control, data-driven control, convex optimisation, bioprocesses

1. Introduction

The exploding demand for cost-effective production of biologic drugs and sustainable production of goods has intensified the need for rapid development and control of bioprocesses (Rathore et al., 2021). This has motivated the development of robotic parallel experimentation facilities capable of performing sophisticated cultivations (e.g. fed-batch, continuous) in high throughput. Some commercially available solutions are the robolector from m2p-labs, bioREACTOR 48 from 2mag, ambr250 from Sartorius, and bioXplorer from H.EL. In the early stages of a project, development is characterised by limited process information and a large experimental design space, posing significant challenges for operating large numbers of bioreactors in parallel (Cruz Bournazou et al., 2017). Adaptive and robust Model Predictive Control (MPC) have been shown to significantly improve process performance and experimental efficiency, even in cases of large uncertainty in model outputs (Krausch et al., 2022; Jabarivelisdeh et al., 2020; Tuveri et al., 2023). However, applications have been restricted to relatively stable process conditions. For example, Kager et al. (2020) were able to increase total product formation in a fungal process, but their approach is limited to the nominal case. The approach of Mowbray et al. (2022) used neural networks (NN) to handle uncertainties but required heavy offline training.

A popular approach in advanced control to deal with uncertain dynamic systems is tube-based MPC (TMPC). Robust nonlinear MPC requires online solution of nonconvex optimisation problems, which can be computationally expensive. A common strategy for applying TMPC to nonlinear systems is to treat the effects of nonlinearity as bounded disturbances and compute successive linear approximations around predicted trajectories (Cannon et al., 2011). These approaches, nevertheless, rely on conservative estimates of linearisation error and can give poor performance (Yu et al., 2013).

Recent studies have shown that tighter bounds on linearisation errors can be achieved if the problem can be expressed as a difference of convex functions (Doff-Sotta and Cannon, 2022; Buerger et al., 2024). This is based on the observation that the necessarily convex linearisation error is maximum at the boundary of the set on which it is evaluated. Tight bounds can thus be derived and incorporated in a robust TMPC formulation. Moreover, the difference of convex functions (DC) structure of the dynamics is attractive as it results in a sequence of convex programs that can be solved with predictable computational effort.

Although any twice continuously differentiable function can be expressed in DC form, finding DC representations can be difficult. To address this issue, we use deep learning NNs with kernel weights constrained to non-negative values and convex, non-decreasing activation functions such as rectified linear units (ReLU, $\sigma(x) = \max(0, x)$), resulting in an input-convex neural network (ICNN) (Amos et al., 2017). The outputs of two ICNNs can be subtracted to learn dynamics in DC form (Sankaranarayanan and Rengaswamy, 2022). Moreover, in the context of TMPC, the tube parameterisation influences the computational complexity of the optimisation prob-

*Corresponding author

Email addresses: niels.krausch@novartis.com (Niels Krausch), martin.doff-sotta@eng.ox.ac.uk (Martin Doff-Sotta), mark.cannon@eng.ox.ac.uk (Mark Cannon), peter.neubauer@tu-berlin.de (Peter Neubauer), mariano.n.cruzournazou@tu-berlin.de (Mariano Nicolas Cruz Bournazou)

lem. Doff-Sotta and Cannon (2022) and Buerger et al. (2024), define tube cross sections using elementwise bounds, but this requires $O(2^{n_x})$ inequality constraints in the MPC optimisation problem (n_x denotes the number of model states), causing significant computational burden for large systems. Simplex tubes, for which the dependence is $O(n_x)$, provide a computationally efficient alternative. This contribution describes a robust TMPC algorithm that leverages deep learning NNs to determine the process dynamics in DC form, implements simplex tubes, enables parameter estimation while providing robustness to parameter uncertainty, and optimises product formation in a case study of a fed-batch bioreactor for the production of penicillin.

2. Modelling and DC approximation using deep learning

We consider a perfectly mixed isothermal fed-batch bioreactor, a popular case study example from (Srinivasan et al., 2003). The model states are the cell concentration X [g L^{-1}], product concentration P [g L^{-1}], substrate concentration S [g L^{-1}] and volume V [L]. The control input is the feed flow rate u [L h^{-1}] of substrate at concentration S_i . The objective of the control strategy is to maximise the product concentration P after a period of T hours while satisfying state and control constraints.

The system model is given by

$$\dot{x} = \phi(x, u) + \xi \quad (1)$$

where $\dot{x} = dx/dt$, $x = (X, S, P, V)$ is the system state and ξ is an unknown bounded disturbance representing measurement noise and parameter errors not explicitly accounted for in the problem description. The function ϕ is defined for $(x, u) \in \mathbb{X} \times \mathbb{U}$, where \mathbb{X}, \mathbb{U} are compact convex state and control constraint sets, by

$$\dot{X} = \mu(S)X - \frac{u}{V_0 + V}X \quad (2a)$$

$$\dot{S} = -\mu(S)\frac{X}{Y_{X/S}} - v\frac{X}{Y_{P/S}} + \frac{u}{V_0 + V}(S_i - S) \quad (2b)$$

$$\dot{P} = vX - \frac{u}{V_0 + V}P \quad (2c)$$

$$\dot{V} = u \quad (2d)$$

$$\mu(S) = \mu_{\max} \frac{S}{S + K_S + S^2/K_i}. \quad (2e)$$

Here μ_{\max} denotes the maximal growth rate (0.02 h^{-1}), K_S is the substrate affinity constant of the cells (0.05 g L^{-1}), K_i is an inhibition constant which inhibits growth at high substrate concentrations (5 g L^{-1}), v is the production rate (0.004 L h^{-1}), the inlet substrate concentration is $S_i = 200 \text{ g L}^{-1}$, $Y_{X/S}$ is the yield coefficient of biomass per substrate ($0.4 \text{ g}_X \text{ g}_S^{-1}$), and $Y_{P/X}$ is the yield coefficient of product per substrate ($1.2 \text{ g}_P \text{ g}_S^{-1}$). The initial volume is $V_0 = 120 \text{ L}$. We assume $Y_{X/S}$ and S_i are unknown to the controller but lie within known intervals as a result of variability in the phenotype of the microorganism and uncertainty in feed concentration due to imperfect measurements or mixing, respectively.

The initial conditions are $X(0) = 1 \text{ g L}^{-1}$, $S(0) = 0.5 \text{ g L}^{-1}$, $P(0) = 0 \text{ g L}^{-1}$, and $V(0) = 0 \text{ L}$, and the constraint sets are

$$\mathbb{X} = \{x : 0 \leq x \leq (3.7, 1, 3, 5)\}, \quad \mathbb{U} = \{u : 0 \leq u \leq 0.2\}. \quad (3)$$

A feedforward deep learning NN framework was used to approximate the dynamics (2a)-(2e) as a difference of convex functions by subtracting the outputs of two feedforward ICNN subnetworks. An ICNN with L layers is characterised by a parameter set $\theta = \{G_{1:L-1}, H_{0:L-1}, b_{0:L-1}\}$ and an input-output map $z_L = f(y; \theta)$, defined for $l = 0, \dots, L-1$ (with $(G_0, z_0) \equiv 0$) by

$$z_{l+1} = \sigma(G_l z_l + H_l y + b_l), \quad (4)$$

where y is the input, z_l is the layer activation, G_l are positively constrained kernel weights ($\{G_l\}_{ij} \geq 0$, for all i, j, l), H_l are input passthrough weights, b_l are bias terms and $\sigma(\cdot)$ is a componentwise convex, nondecreasing activation function. We use ReLU activation functions: $\sigma(\xi) = \max(\xi, 0)$. Each network layer thus consists of the composition of a linear (and hence convex) function with a nondecreasing convex function, so $z_L = f(y; \theta)$ is necessarily a convex map from y to z_L . We define $y = (x, u)$ and use z_L to approximate the map $\phi(x, u)$, where $x = (X, S, P, V)$ and u are the state and control input of the system (1). Two ICNNs whose outputs are subtracted are trained simultaneously to learn the dynamics of (1) as a difference of convex functions:

$$\dot{x} = f_1(x, u) - f_2(x, u) + \zeta, \quad (5)$$

where ζ is an unknown but bounded disturbance that accounts for the approximation errors in f_1, f_2 and the disturbance ξ in (1). Each of the two ICNNs consists of an input layer, two hidden layers with 32 nodes each, and an output layer. Thus $\phi(x, u)$ in (1) is approximated by $G_{2,1}z_{2,1} - G_{2,2}z_{2,2}$ where $z_{2,i}$ for $i = 1$ or 2 has the form of (4) with $L = 2$.

The network was implemented using Keras (Chollet et al., 2015) and trained over 250 epochs with the RMSProp optimiser using 10^5 random samples of the right-hand sides of (2a)-(2d), which were divided into 80% training and 20% validation sets. To enable evaluation of each sampling point, the unknown parameters $Y_{X/S}, S_i$ were set to nominal values, denoted $\bar{Y}_{X/S}, \bar{S}_i$. Convexity of the models was evaluated by checking the Hessian matrices: $\nabla^2 f_i(x, u) \geq 0$, $i = 1, 2$, at all points (x, u) in the validation set. Figure 1 shows the DC decompositions representing \dot{X} and \dot{S} for given values of P, V , and u . As illustrated, the NN provides obtain a good fit (MAE: 0.0012) for the model (2) (blue dots and blue surface), and the DC form of the decomposition is apparent in Fig. 1 (orange and green surfaces).

3. DC-TMPC framework with simplexes

Doff-Sotta and Cannon (2022) proposed a robust TMPC algorithm based on successive linearisation for DC systems. The so-called DC-TMPC algorithm capitalises on the idea that optimisation problems with inequality constraints involving DC functions can be approximated as convex problems by linearising only the concave parts of the inequality constraints. Furthermore, bounds on the errors introduced by linearising concave functions are trivial to compute and can be treated as disturbances in a robust TMPC scheme. We apply this approach to the system (5) learned in DC form with additive disturbances, and we extend it by considering state tubes defined in terms of simplexes in order to reduce online computational load.

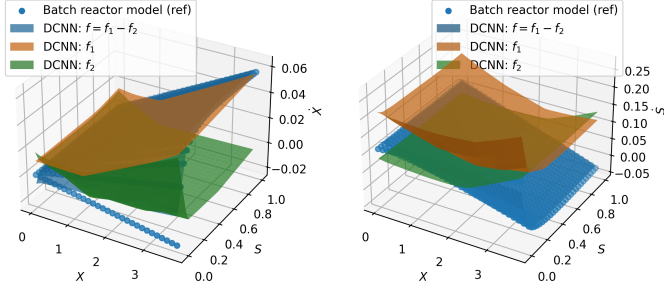


Figure 1: DC decomposition: the actual model evaluated at 30×30 sample points (blue dots), the convex functions f_1 and f_2 (orange and green surfaces), and the DC decomposition $f = f_1 - f_2$ (blue surfaces) approximating \dot{X} (left), and \dot{S} (right), as functions of the concentrations X and S , with product concentration $P = 0.4 \text{ g L}^{-1}$, volume $V = 122 \text{ L}$, and feed rate $u = 0.07 \text{ L h}^{-1}$.

We can derive a discrete time model from (5) using, for example, forward Euler approximation:

$$x_{k+1} = \delta(f_1(x_k, u_k) - f_2(x_k, u_k)) + w_k, \quad (6)$$

where y_k denotes the value of variable y at discrete time index $k \in \{0, 1, 2, \dots\}$ and the sampling interval is $\delta = 1$ hour. The disturbance w_k lies in a bounded set \mathbb{W} for all k , where \mathbb{W} can be estimated using data on the disturbance affecting the continuous time system (1) and the error in its DC approximation in (5).

The tube MPC strategy is based on linearising f_1 and f_2 in (6) around nominal predicted trajectories $\{x_k^\circ, u_k^\circ\}_{k=0:N}$ over a future horizon of N discrete time steps. For a given control sequence $\{u_k^\circ\}_{k=0:N}$, we compute $\{x_k^\circ\}_{k=0:N}$ by applying an ODE solver to the model (1) with nominal parameters (i.e. $\xi = 0$, $Y_{X/S} = \bar{Y}_{X/S}$, $S_i = \bar{S}_i$). We denote the state and input perturbations relative to x_k°, u_k° as $s_k = x_k - x_k^\circ$ and $v_k = u_k - u_k^\circ$ respectively. To reduce the effects of model uncertainty on predicted trajectories, v_k is defined by a two degree-of-freedom control law: $v_k = K_k s_k + c_k$, where $\{K_k\}_{k=0:N}$ are feedback gains and $\{c_k\}_{k=0:N}$ is a feedforward control sequence computed at each discrete time step by solving a sequence of convex optimisation problems.

Bounds on the predicted trajectories of the model (6) are obtained by exploiting the componentwise convexity of f_i , $i = 1, 2$, which implies that each component of f_i is upper-bounded by the Jacobian linearisation of f_i about any point in its domain. This provides the following bounds, which are by construction convex conditions on $\{s_k\}_{k=0:N}$ and $\{c_k\}_{k=0:N}$,

$$s_{k+1} \geq s_k + \delta(f_1(x_k^\circ + s_k, u_k^\circ + v_k) - f_1(x_k^\circ, u_k^\circ)) - F_{2,k} s_k - B_{2,k} c_k + \delta \max_{w \in \mathbb{W}} w_k \quad (7a)$$

$$s_{k+1} \leq s_k + F_{1,k} s_k + B_{1,k} c_k - \delta(f_2(x_k^\circ + s_k, u_k^\circ + v_k) - f_2(x_k^\circ, u_k^\circ)) + \delta \min_{w \in \mathbb{W}} w_k \quad (7b)$$

where $F_{i,k} = \delta(A_{i,k} + B_{i,k}K)$, $A_{i,k} = \frac{\partial f_i}{\partial x}(x_k^\circ, u_k^\circ)$, $B_{i,k} = \frac{\partial f_i}{\partial u}(x_k^\circ, u_k^\circ)$ for $i = 1, 2$.

To ensure robust constraint satisfaction and convergence of the successive linearisation scheme, we define an uncertainty tube consisting of a sequence of sets $\{\mathbb{S}_k\}_{k=0:N}$ bounding the state perturbation trajectories under all realisations of model

uncertainty. The tube $\{\mathbb{S}_k\}_{k=0:N}$ may be defined in terms of componentwise bounds (e.g. Doff-Sotta and Cannon, 2022), but the number of constraints needed then grows exponentially with the state dimension n_x . To reduce this to a linear dependence, we instead parameterise $\{\mathbb{S}_k\}_{k=0:N}$ in terms of simplexes:

$$\mathbb{S}_k = \left\{ s \in \mathbb{R}^{n_x} : \begin{bmatrix} -I \\ \mathbf{1}^\top \end{bmatrix} s \leq \begin{bmatrix} \alpha_k \\ \beta_k \end{bmatrix} \right\} \quad (8)$$

where $I \in \mathbb{R}^{n_x \times n_x}$ is the identity matrix, $\mathbf{1}$ is a vector of ones, and the vector α_k and scalar β_k are optimisation variables. Conditions on $\{\alpha_k, \beta_k\}_{k=0:N}$ to ensure that the state perturbation s_k belongs to \mathbb{S}_k for all $k \in \{0, \dots, N\}$ can be defined recursively as follows. Combining (7) and (8), we require, for all $s \in \mathbb{S}_k$, $k = 0, 1, \dots, N-1$,

$$\alpha_{k+1} \geq \max_{s \in \mathbb{S}_k} \left(-s + \delta f_2(x_k^\circ + s, u_k^\circ + K_k s + c_k) - \delta f_2(x_k^\circ, u_k^\circ) - F_{1,k} s - B_{1,k} c_k \right) - \delta \min_{w \in \mathbb{W}} w \quad (9a)$$

$$\beta_{k+1} \geq \max_{s \in \mathbb{S}_k} \mathbf{1}^\top \left(s + \delta f_1(x_k^\circ + s, u_k^\circ + K_k s + c_k) - \delta f_1(x_k^\circ, u_k^\circ) - F_{2,k} s - B_{2,k} c_k \right) + \delta \max_{w \in \mathbb{W}} \mathbf{1}^\top w \quad (9b)$$

The conditions in (9a)-(9b) can be equivalently expressed in terms of $n_x + 1$ convex inequalities using the set of vertices of \mathbb{S}_k , denoted $\{s_k^j\}_{j=0:n_x}$, which are given in terms of α_k, β_k as

$$s_k^j = \begin{cases} -\alpha_k & j = 0 \\ -\alpha_k + (\beta_k + \mathbf{1}^\top \alpha_k) e_j & j = 1, \dots, n_x \end{cases} \quad (10)$$

where e_j is the j th column of the identity matrix in $\mathbb{R}^{n_x \times n_x}$. Exploiting again the convexity of f_1 and f_2 , conditions (9a)-(9b) are therefore equivalent to the constraints, for $j = 0, 1, \dots, n_x$:

$$\begin{aligned} \alpha_{k+1} &\geq -s_k^j + \delta f_2(x_k^\circ + s_k^j, u_k^\circ + K_k s_k^j + c_k) - \delta f_2(x_k^\circ, u_k^\circ) \\ &\quad - F_{1,k} s_k^j - B_{1,k} c_k - \delta w_{\min} \\ \beta_{k+1} &\geq \mathbf{1}^\top \left(s_k^j + \delta f_1(x_k^\circ + s_k^j, u_k^\circ + K_k s_k^j + c_k) - \delta f_1(x_k^\circ, u_k^\circ) \right. \\ &\quad \left. - F_{2,k} s_k^j - B_{2,k} c_k \right) + \delta w_{\max} \end{aligned}$$

where w_{\min}, w_{\max} are defined by $e_i^\top w_{\min} = \min_{w \in \mathbb{W}} e_i^\top w$ for $i = 1, \dots, n_x$, $w_{\max} = \max_{w \in \mathbb{W}} \mathbf{1}^\top w$.

4. MPC algorithm for no parameter uncertainty

This section considers the case in which the parameters of (2) are known to the controller but the model (1) is affected by unknown bounded disturbances. We therefore assume that the discrete time model (6) has no parametric uncertainty (in particular $Y_{X/S}$ and S_i are equal to their nominal values $\bar{Y}_{X/S}, \bar{S}_i$), but is subject to disturbances with known bounds $\mathbb{W} \ni w_k$ for all k . At each sampling instant $t = 0, \delta, 2\delta, \dots$, given the current state $x(t)$ of (2), we optimise the feedforward sequence $\{c_k\}_{k=0:N}$ and tube parameters $\{\alpha_k, \beta_k\}_{k=0:N}$ subject to (9a,b) and $x_k \in \mathbb{X}$, $u_k \in \mathbb{U}$ for all k by solving the following convex problem

$$\underset{c_k, \alpha_k, \beta_k, k=0, \dots, N}{\text{maximize}} \sum_{k=0}^N (l_{x,k} - \gamma l_{u,k}) \quad (11a)$$

subject to, for all $k \in \{0, \dots, N-1\}$ and $j \in \{0, \dots, n_x\}$

$$x_k^\circ + s_k^j \in \mathbb{X}, \quad u_k^\circ + K s_k^j + c_k \in \mathbb{U} \quad (11b)$$

$$\alpha_{k+1} \geq -s_k^j + \delta f_2(x_k^\circ + s_k^j, u_k^\circ + K s_k^j + c_k) - \delta f_2(x_k^\circ, u_k^\circ) - F_{1,k} s_k^j - B_{1,k} c_k - \delta w_{\min} \quad (11c)$$

$$\beta_{k+1} \geq \underline{1}^\top (s_k^j + \delta f_1(x_k^\circ + s_k^j, u_k^\circ + K s_k^j + c_k) - \delta f_1(x_k^\circ, u_k^\circ) - F_{2,k} s_k^j - B_{2,k} c_k) + \delta w_{\max} \quad (11d)$$

$$l_{x,k} \leq \underline{e}_3^\top (x_k^\circ + s_k^j) \quad (11e)$$

$$l_{u,k+1} \geq (u_{k+1}^\circ + K s_{k+1}^j + c_{k+1} - u_k^\circ - K s_k^j - c_k)^2 \quad (11f)$$

and the initial constraints, for all $j \in \{0, \dots, n_x\}$

$$l_{u,0} \geq (u_0^\circ + K s_0^j + c_0 - u(t-\delta))^2 \quad (11g)$$

$$\alpha_0 \geq x_0^\circ - x(t) \quad (11h)$$

$$\beta_0 \geq \underline{1}^\top (x(t) - x_0^\circ) \quad (11i)$$

and terminal constraints for all $k \in \{0, \dots, N_{\text{term}}\}$, $j \in \{0, \dots, n_x\}$

$$c_{N-k} = 0 \quad (11j)$$

$$x_{N-k}^\circ + s_{N-k}^j \leq x_{\text{term}}. \quad (11k)$$

A brief explanation of the problem formulation is as follows.

- The objective function (11a) aims to maximise the product concentration via the term $l_{x,k}$, which is a lower bound on $P = \underline{e}_3^\top x$ due to (11e). The term $l_{u,k}$ smooths the solution by penalising changes in the control input via (11f,g). The scalar constant γ balances these two competing objectives.
- The state and control constraints in (11b) depend on the sets \mathbb{X} , \mathbb{U} defined in (3). By definition all model states and control inputs must be non-negative, while the upper bounds $u \leq 0.2$ and $x \leq (3.7, 1, 3, 5)$ are context-specific.
- The tube constraints (11c,d) are equivalent to (9a,b) and, with s_k^j defined in (10), ensure that $s_k \in \mathbb{S}_k$ for $1 \leq k \leq N$.
- The initial constraints (11i,j) ensure $s_0 = x(t) - x_0^\circ \in \mathbb{S}_0$.
- The terminal constraints (11k,l) allow for a guarantee that problem (11) remains feasible for all $t > 0$ if it is feasible at $t = 0$. Here N_{term} and $x_{\text{term}} \in \mathbb{X}$ are chosen so that the set $\{x_0 : x_k \leq x_{\text{term}}, k = 0, \dots, N_{\text{term}}\}$ is positively invariant.

If the substrate concentration S remains low for an extended period, the bioreactor effectively shuts down due to the depletion of the main carbon source. Using data from simulations of (1)-(2), we identify this condition as $S \leq 0.1 \text{ g L}^{-1}$ for a period of 5 hours, and hence we define $x_{\text{term}} = (3.7, 0.1, 3, 5)$ and $N_{\text{term}} = 5$ in the terminal constraints (11k,l).

The solution, denoted $\{c_k^*\}_{k=0:N}$, of (11) is used to update the state and input trajectories $\{x_k^\circ, u_k^\circ\}_{k=0:N}$ to be employed at the next iteration by setting $s_0 \leftarrow x(t) - x_0^\circ$ and for $k = 0, 1, \dots, N$:

$$u_k^\circ \leftarrow u_k^\circ + K_k s_k + c_k^* \quad (12a)$$

$$s_{k+1} \leftarrow \Phi(x_k^\circ, u_k^\circ) - x_{k+1}^\circ \quad (12b)$$

$$x_{k+1}^\circ \leftarrow \Phi(x_k^\circ, u_k^\circ) \quad (12c)$$

where $\Phi(x_k, u_k)$ is the solution for x_{k+1} obtained from (1) under nominal conditions ($\xi = 0$, $Y_{X/S} = \bar{Y}_{X/S}$, $S_i = \bar{S}_i$) using an ODE solver (e.g. cvodes (Hindmarsh et al., 2005) implemented in CasADi (Andersson et al., 2019)).

The optimisation (11) and update (12) are repeated until the control perturbation $\sum_k \|c_k^*\|$ and change in optimal cost fall below given thresholds, or until a maximum number of iterations is reached. The control input is then applied to the bioreactor as $u(\tau) = u_0^\circ$ for $\tau \in [t, t+\delta)$. At the next sampling instant, $t+\delta$, we set $x_0^\circ = x(t+\delta)$ and redefine $\{u_k^\circ, x_k^\circ\}_{k=0:N}$ using the optimal solution at the final iteration of time t by setting $s_0 \leftarrow 0$ and

$$u_k^\circ \leftarrow u_{k+1}^\circ + K_{k+1} s_k + c_{k+1}^*, \quad k = 0, 1, \dots, N-1 \quad (13a)$$

$$s_{k+1} \leftarrow \Phi(x_k^\circ, u_k^\circ) - x_{k+1}^\circ, \quad k = 0, 1, \dots, N \quad (13b)$$

$$x_{k+1}^\circ \leftarrow \Phi(x_k^\circ, u_k^\circ), \quad k = 0, 1, \dots, N \quad (13c)$$

with $u_{N+1}^\circ \leftarrow u^r$, where u^r is such that $x(t) \leq x_{\text{term}}$ for all $t > 0$ if $x(0) \leq x_{\text{term}}$ and $u(t) = u^r$. With $x_{\text{term}} = (3.7, 0.1, 3, 5)$ we find $u^r = 0.01 \text{ L h}^{-1}$ meets this requirement for the system (1).

Since (12) and (13) use the nominal system model to update $\{u_k^\circ, x_k^\circ\}_{k=0:N}$, it cannot be guaranteed that the updated trajectory will result in a feasible updated problem (11). An alternative update strategy that provides a guarantee of feasibility is proposed in Lishkova and Cannon (2025). However, we use here a simpler approach, exploiting the observation that the nominal trajectory $\{u_k^\circ, x_k^\circ\}_{k=0:N}$ computed at a feasible previous iteration necessarily provides a set of linearisation points such that problem (11) is feasible at the current iteration. This is a direct consequence of the tube $\{\mathbb{S}_k\}_{k=0:N}$ containing the state trajectories for all possible uncertainty realisations. Thus, if (11) is infeasible after the update (13), we instead define $\{x_k^\circ, u_k^\circ\}_{k=0:N}$ as a time-shifted version of the previous nominal trajectory:

$$u_k^\circ \leftarrow u_{k+1}^\circ, \quad k = 0, 1, \dots, N-1 \quad (14a)$$

$$x_k^\circ \leftarrow x_{k+1}^\circ, \quad k = 0, 1, \dots, N \quad (14b)$$

$$u_N^\circ \leftarrow u^r \quad (14c)$$

$$x_{N+1}^\circ \leftarrow \Phi(x_k^\circ, u_N^\circ) \quad (14d)$$

The update strategy in (12)-(14) ensures that (11) is recursively feasible, i.e. a feasible solution of (11) is obtained at each iteration and for all $t > 0$ if (11) is feasible at $t = 0$. The algorithm can be initialised at $t = 0$ by setting $x_0^\circ = x(0)$, $u_k^\circ = u^r$ and $c_k^* = 0$ for all k , and computing $\{x_k^\circ\}_{k=1:N}$ using (12).

By construction, the DC-TMPC strategy satisfies the constraints $x(n\delta) \in \mathbb{X}$, $u(n\delta) \in \mathbb{U}$ for $n = 0, 1, \dots$ regardless of the number of iterations performed at each time step. Hence computation can be reduced to a single solution of the convex problem (11) at each time step. On the other hand, if there is no limit on the number of iterations, then for the limiting case of no model uncertainty ($\mathbb{W} \rightarrow \{0\}$), the DC-TMPC iteration converges to an optimal solution for the problem of maximising product concentration for the system (1)-(2) subject to $(x, u) \in \mathbb{X} \times \mathbb{U}$ (see Lishkova and Cannon, 2025).

5. Adaptive MPC algorithm for parameter uncertainty

This section discusses robust adaptive DC-TMPC subject to parameter uncertainty and unknown disturbances with known bounds. Since the uncertain parameters S_i and $Y_{X/S}^{-1}$ appear linearly in the bioreactor model (2), we can write the system model (1) in a form that depends linearly on an unknown parameter vector θ ,

$$\dot{x} = \phi(x, u) + \underline{e}_2 \psi(x, u)^\top \theta + \xi. \quad (15)$$

Here $\phi(x, u)$ is defined by (2a)-(2e) with $Y_{X/S}, S_i$ replaced by their nominal values $\bar{Y}_{X/S}, \bar{S}_i$, and $\psi(x, u)$ and θ are the vectors

$$\psi(x, u) = \begin{bmatrix} -\mu(S)X \\ 100u/(V + V_0) \end{bmatrix}, \quad \theta = \begin{bmatrix} Y_{X/S}^{-1} - \bar{Y}_{X/S}^{-1} \\ (S_i - \bar{S}_i)/100 \end{bmatrix}.$$

Extending the approach of Sections 2, 3 and 4 to account for uncertainty in θ , we propose a robust DC-TMPC strategy for controlling (15). This is combined with online estimation of θ to create a robust adaptive control algorithm.

Analogously to the DC model (6), we construct a DC representation $\psi(x, u) = g_1(x, u) - g_2(x, u)$, where $g_i(x, u)$ for $i = 1, 2$ is componentwise convex in (x, u) , using the difference of two ICNNs. For this example we use feedforward NNs with the same structure as the ICNNs described in Section 2, but with 16 nodes in each hidden layer. The ICNNs were trained simultaneously on samples of the map $\psi(x, u)$ without knowledge of the true parameter values. Combining this model with (6), which was identified using the nominal parameters $\bar{Y}_{X/S}, \bar{S}_i$, we obtain

$$\begin{aligned} x_{k+1} &= \delta(f_1(x_k, u_k) - f_2(x_k, u_k)) \\ &+ \delta \underline{e}_2 (g_1(x_k, u_k) - g_2(x_k, u_k))^\top \theta + w_k. \end{aligned} \quad (16)$$

A set \mathbb{W} bounding the disturbance w_k can be constructed from bounds on the disturbance affecting the system (1) and the approximation errors in the DC representations of ϕ and ψ .

An initial bounding set Θ_0 containing θ can be determined if prior parameter bounds are available. For example, with nominal parameter values $\bar{Y}_{X/S} = 0.45$, $\bar{S}_i = 195 \text{ g L}^{-1}$ and bounds $Y_{X/S} \in [0.333, 0.5]$, $S_i \in [180, 220]$, we obtain

$$\theta \in \Theta_0 = \{\theta : (-0.222, -0.15) \leq \theta \leq (0.778, 0.25)\},$$

and the actual parameter values $Y_{X/S} = 0.4$, $S_i = 200 \text{ g L}^{-1}$ imply $\theta^* = (0.278, 0.05)$ is the true value of θ .

We use online set membership estimation (Lorenzen et al., 2019; Lu et al., 2021) to update bounds on θ using online state measurements and prior disturbance bounds. At time $t = n\delta$, for $n = 0, 1, \dots$, the parameter set $\Theta_n = \{\theta : H\theta \leq h_n\}$ is defined in terms of a vector h_n that is updated online and a constant matrix H that is chosen offline so that Θ_n has a fixed number of vertices. Thus if $H = [I \ -I]^\top$ so that h_n determines upper and lower bounds on the elements of θ , then Θ_n has 4 vertices. Let $D_n = D(x_n, u_n) = \delta \underline{e}_2 (g_1(x_n, u_n) - g_2(x_n, u_n))^\top$ and $d_n = d(x_n, u_n) = \delta(f_1(x_n, u_n) - f_2(x_n, u_n))$. Then (16) can be written as $x_{n+1} = D_n \theta + d_n + w_n$, and at time step $n+1$, θ must belong to an unfalsified parameter set given by $\{\theta : x_{n+1} - d_n - D_n \theta \in \mathbb{W}\}$.

Hence, using observations of x_n over a window of N_{est} discrete time steps, we update Θ_n by solving a linear program:

$$\begin{aligned} h_{n,i} &= \max_{\theta \in \Theta_{n-1}} H_i \theta \\ &\text{subject to } x_{n-k+1} - d_{n-k} - D_{n-k} \theta \in \mathbb{W}, \quad \forall k \in \{1, \dots, N_{\text{est}}\} \end{aligned}$$

for each element i of h_n , where $h_{n,i}, H_i$ are the i th element and i th row of h_n, H . This update rule ensures that $\Theta_n \subseteq \dots \subseteq \Theta_0$ and Θ_n converges asymptotically to the true parameter vector θ^* if the control input is persistently exciting (Lu et al., 2021).

We also compute a point estimate $\hat{\theta}_n$ online using Least Mean Squares (LMS) (Lorenzen et al., 2019). Given the nominal 1-step ahead prediction from (16), $\hat{x}_{1|n} = D_n \hat{\theta}_n + d_n$, and the actual system state x_{n+1} , the estimate is updated at discrete time $n+1$ via

$$\hat{\theta}_{n+1} = \Pi_{\Theta_{n+1}}[\hat{\theta}_n + \hat{\mu} D_n^\top (x_{n+1} - \hat{x}_{1|n})]$$

where $\Pi_{\Theta}[\cdot]$ denotes the (Euclidean) projection onto Θ , and $\hat{\mu}$ is an update gain satisfying $\frac{1}{\hat{\mu}} > \|D(x, u)\|^2$ for all $(x, u) \in \mathbb{X} \times \mathbb{U}$.

The parameter set estimate Θ_n can be used to make the DC-TMPC optimisation (11) robust to parameter uncertainty, while the point estimate $\hat{\theta}_n$ can improve the accuracy of the nominal predicted trajectories $\{x_k^\circ, u_k^\circ\}_{k=0:N}$ at sampling instant $t = n\delta$. These modifications result in an adaptive DC-MPC algorithm with improved robustness to model uncertainty and potentially better performance than the strategy outlined in Section 4, albeit at the expense of increased computation.

In particular, when computing the nominal predicted trajectories $\{x_k^\circ, u_k^\circ\}_{k=0:N}$ the map $\Phi(x, u)$ in (12)-(14) is determined by solving (1) with $\xi = 0$ and the current parameter estimates

$$Y_{X/S} = (\hat{\theta}_{n,1} + \bar{Y}_{X/S}^{-1})^{-1}, \quad S_i = 100 \hat{\theta}_{n,2} + \bar{S}_i,$$

where $\hat{\theta}_n = (\hat{\theta}_{n,1}, \hat{\theta}_{n,2})$. In addition, the tube $\{x_k^\circ + \mathbb{S}_k\}_{k=0:N}$ necessarily contains the system state under all model possible uncertainty realisations when constraints (11c,d) are replaced by

$$\begin{aligned} \alpha_{k+1} &\geq -s_k^j + \delta f_2(x_k^\circ + s_k^j, u_k^\circ + K_k s_k^j + c_k) - \delta f_2(x_k^\circ, u_k^\circ) \\ &- (F_{1,k} s_k^j + B_{1,k} c_k) - \delta w_{\min} \\ &+ \underline{e}_2 \theta_+^{m\top} (\delta g_2(x_k^\circ + s_k^j, u_k^\circ + K_k s_k^j + c_k) - \delta g_2(x_k^\circ, u_k^\circ)) \\ &- \underline{e}_2 \theta_+^{m\top} (G_{1,k} s_k^j + B_{1,k}^g c_k) \\ &- \underline{e}_2 \theta_-^{m\top} (\delta g_1(x_k^\circ + s_k^j, u_k^\circ + K_k s_k^j + c_k) - \delta g_1(x_k^\circ, u_k^\circ)) \\ &+ \underline{e}_2 \theta_-^{m\top} (G_{2,k} s_k^j + B_{2,k}^g c_k) \end{aligned} \quad (17a)$$

$$\begin{aligned} \beta_{k+1} &\geq \underline{1}^\top (s_k^j + \delta f_1(x_k^\circ + s_k^j, u_k^\circ + K_k s_k^j + c_k) - \delta f_1(x_k^\circ, u_k^\circ)) \\ &- \underline{1}^\top (F_{2,k} s_k^j + B_{2,k} c_k) + \delta w_{\max} \\ &+ \theta_+^{m\top} (\delta g_1(x_k^\circ + s_k^j, u_k^\circ + K_k s_k^j + c_k) - \delta g_1(x_k^\circ, u_k^\circ)) \\ &- \theta_+^{m\top} (G_{2,k} s_k^j + B_{2,k}^g c_k) \\ &- \theta_-^{m\top} (\delta g_2(x_k^\circ + s_k^j, u_k^\circ + K_k s_k^j + c_k) - \delta g_2(x_k^\circ, u_k^\circ)) \\ &+ \theta_-^{m\top} (G_{1,k} s_k^j + B_{1,k}^g c_k). \end{aligned} \quad (17b)$$

Here $G_{i,k} = \delta(A_{i,k}^g + B_{i,k}^g K)$, $A_{i,k}^g = \frac{\partial g_i}{\partial x}(x_k^\circ, u_k^\circ)$, $B_{i,k}^g = \frac{\partial g_i}{\partial u}(x_k^\circ, u_k^\circ)$ for $i = 1, 2$, and $\{\theta^m\}_{m=1:4}$ are the vertices of Θ_n , with

$$\theta_+^m = \max\{\theta^m, 0\}, \quad \theta_-^m = \min\{\theta^m, 0\}$$

denoting the non-negative and non-positive components of θ^m .

Problem (11), with (17a,b) replacing (11c,d), and with $\{x_k^o, u_k^o\}_{k=0:N}$ updated via (12)-(14), is necessarily recursively feasible since $\Theta_{n+1} \subseteq \Theta_n$ for all $n \geq 0$. In addition, the closed loop adaptive DC-TMPC strategy ensures satisfaction of the constraints $(x(t), u(t)) \in \mathbb{X} \times \mathbb{U}$ at all sampling instants $t = n\delta$, $n = 0, 1, \dots$. These properties hold regardless of the number of iterations performed at each time step, allowing computationally efficient implementations of the controller. Convergence of the parameter set and pointwise estimates is not guaranteed for the DC-TMPC algorithm as stated here, although techniques for ensuring persistence of excitation (e.g. Lu and Cannon, 2023) could be incorporated into the approach.

6. Simulation results and discussion

The control algorithm was implemented in simulations of the fed-batch bioreactor described in Section 2. The control objective is to maximise product concentration over a period of $T = 100$ h subject to constraints (3). Two pairs of ICNNs were trained as described in Sections 2 and 5 to provide a DC model representation, and the DC-TMPC algorithm was formulated as described in Sections 4 and 5. The online optimisation (11), (17a,b) is a (convex) second order cone program (SOCP) since the constraint sets \mathbb{X}, \mathbb{U} are polytopic and the ICNNs employ ReLU (piecewise linear) activation functions. We solve this problem using *cvxpy* (Diamond and Boyd, 2016) to interface the *gurobi* solver (Gurobi Optimization, LLC, 2023). Model linearisation was performed using TensorFlow and Keras.

We use a prediction horizon of $N = 25$ time steps and cost weight $\gamma = 0.1$ in (11a). Based on the ICNN validation data, the disturbance bounds are given by

$$\mathbb{W} = \{w : |w| \leq (10^{-2}, 10^{-3}, 10^{-3}, 10^{-2})\}.$$

The gains $\{K_k\}_{k=0:N}$ were found by solving the linear quadratic regulator problem defined by the time-varying linearised model around nominal predicted trajectories with $Q = 10^{-5}I, R = 1$.

For the DC-TMPC algorithm of Section 4 without parameter uncertainty, a single iteration requires on average 1.0 s and at most 1.2 s (Apple M3 Pro, 36 GB memory). When parameter uncertainty is included as described in Section 5 the computation time increases to 12 s on average and maximum 15 s.

Predicted trajectories computed at the first time step ($t = 0$) are shown in Fig. 2. Convergence was reached after 10 iterations (at which point the changes in optimal cost and optimal solution for $\{c_k\}_{k=0:N}$ were below the chosen thresholds of 10^{-3} and 10^{-4} respectively). The nominal trajectories (solid lines) can be seen to lie within the bounds on future states provided by the predicted tubes (dashed and dash-dotted lines), which is expected since the tubes provide robust bounds on the state trajectories despite the presence of uncertain parameters and unknown disturbances. The effect of the terminal constraint, requiring $S_k \leq 0.01$ for $20 \leq k \leq 25$, can also be seen.

The closed loop state and control trajectories over 100 time steps are shown in Fig. 3. The constraints on biomass ($X \leq 3.7$) and substrate concentration $S \geq 0$ are active towards the end

of the simulation. Figure 3 also shows the parameter estimate $\hat{\theta}_t$ (green lines) and the estimated parameter bounds corresponding to Θ_t (orange and blue lines). Although the parameter set shrinks over time, convergence is slow after the first 10 time steps due to the unexciting optimal control trajectory in Fig. 3. The rate of convergence of parameter estimates improves when random noise (independent, uniformly distributed within bounds of $\pm 10^{-2}$) is added to the control sequence, as shown in Figure 4. The resulting trajectories are more noisy and the improvement in parameter estimate accuracy is accompanied by a reduction in final product concentration, which falls from 0.96 in Fig. 3 to 0.93 in Fig. 4. The presented DC-TMPC algorithm improves on the multi-stage NMPC of Lucia and Engell (2013) for this case study in terms of computation and performance, and by enabling online parameter estimation.

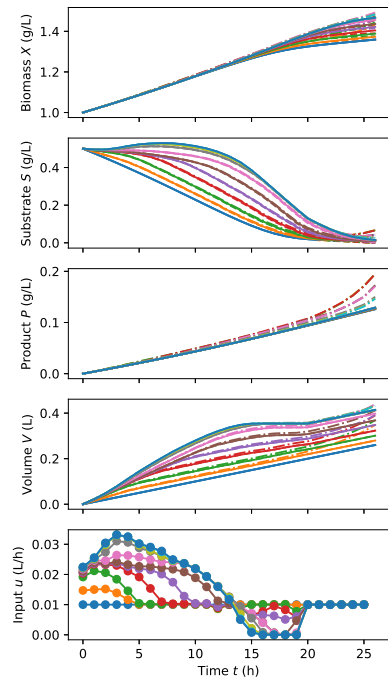


Figure 2: Predicted state and control trajectories at initial time, $t = 0$. Solid lines: nominal predicted trajectories $\{x_k^o, u_k^o\}_{k=0:N}$, dashed/dash-dotted lines: lower/upper bounds on predicted states within $\{S_k\}_{k=0:N}$.

7. Conclusion

This study demonstrates the potential of deep learning robust tube MPC for optimising a bioprocess with uncertain model parameters and disturbances. Our approach uses differences of convex (DC) functions to represent the system dynamics, and explains how to obtain these systematically using deep learning neural networks. With this problem formulation, future performance can be optimised by solving a sequence of convex problems in which model linearisation errors appear as bounded disturbances. Crucially, by convexity, the bounds on these errors are tight and the resulting controller is less conservative than classical TMPC based on successive linearisation. The main contributions of this paper are the demonstration of a method using ReLU NNs for computing DC decompositions, the implementation of simplex tubes, the development of robust adap-

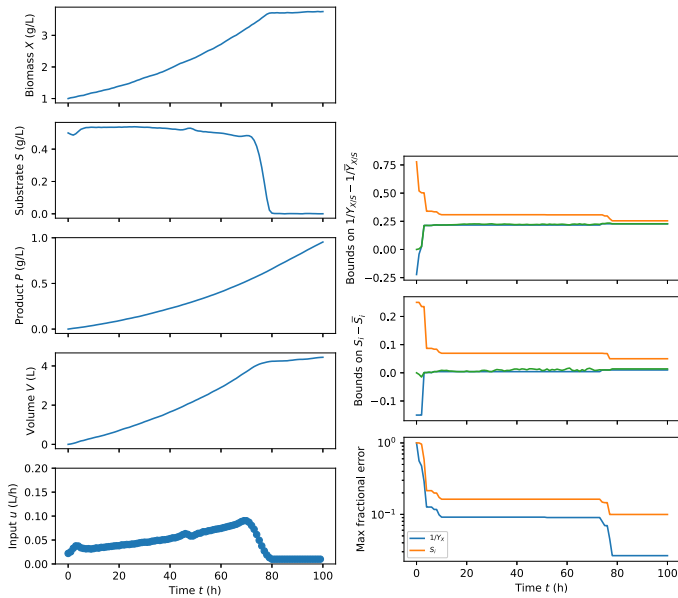


Figure 3: Closed loop state and control trajectories (left) and parameter estimates (right).

tive MPC leveraging DC models with online set membership and least mean squares estimators, and the application of these techniques within a bioreactor case-study. Future work will incorporate more complex models and testing on a real parallel bioreactor system for bioprocess development of different host organisms and products.

Acknowledgments: We gratefully acknowledge the financial support of the German Federal Ministry of Education and Research (BMBF) (ref. 01DD20002A-KIWI Biolab) and the EP-SRC (UKRI) Doctoral Prize scheme (ref. EP/W524311/1).

References

- Amos, B., Xu, L., Kolter, J.Z., 2017. Input convex neural networks, in: Proceedings of the 34th International Conference on Machine Learning, PMLR. pp. 146–155.
- Andersson, J.A.E., Gillis, J., Horn, G., Rawlings, J.B., Diehl, M., 2019. CasADi – A software framework for nonlinear optimization and optimal control. *Mathematical Programming Computation* 11, 1–36.
- Buerger, J., Cannon, M., Doff-Sotta, M., 2024. Safe learning in nonlinear model predictive control, in: Proceedings of the 6th Annual Learning for Dynamics and Control (L4DC), PMLR. pp. 603–614.
- Cannon, M., Buerger, J., Kouvaritakis, B., Rakovic, S., 2011. Robust tubes in nonlinear model predictive control. *IEEE Transactions on Automatic Control* 56, 1942–1947.
- Chollet, F., et al., 2015. Keras. <https://keras.io>.
- Cruz Bourmazou, M., Barz, T., Nickel, D., Lopez Cárdenas, D., Glauche, F., Knepper, A., Neubauer, P., 2017. Online optimal experimental re-design in robotic parallel fed-batch cultivation facilities. *Biotechnology and Bioengineering* 114, 610–619.
- Diamond, S., Boyd, S., 2016. CVXPY: A Python-embedded modeling language for convex optimization. *J Mach Learn Res* 17, 1–5.
- Doff-Sotta, M., Cannon, M., 2022. Difference of convex functions in robust tube nonlinear MPC, in: 61st IEEE Conference on Decision and Control, Cancun, pp. 3044–3050.
- Gurobi Optimization, LLC, 2023. Gurobi Optimizer Reference Manual. URL: <https://www.gurobi.com>.
- Hindmarsh, A., Brown, P., Grant, K., Lee, S., Serban, R., Shumaker, D., Woodward, C., 2005. SUNDIALS, suite of nonlinear and differential/algebraic equation solvers. *ACM Trans. Math. Softw.* 31, 363–396.

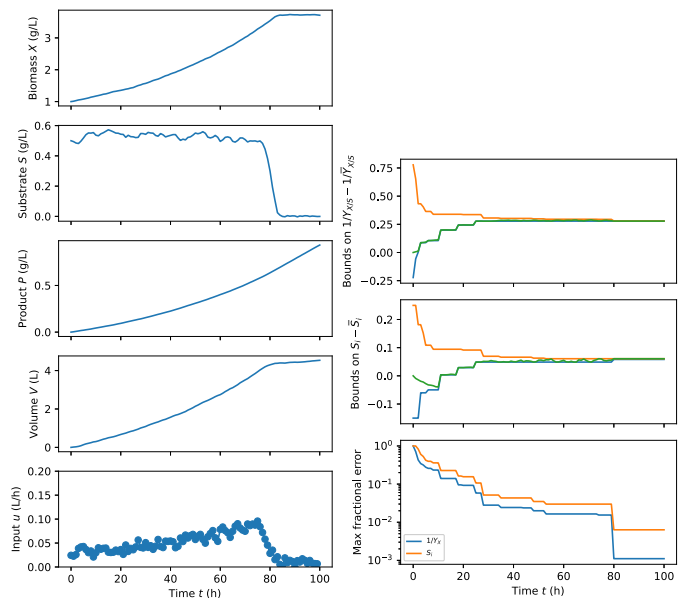


Figure 4: Closed loop state and control trajectories with noisy inputs (left) and parameter estimates (right).

- Jabarivelisdeh, B., Carius, L., Findeisen, R., Waldherr, S., 2020. Adaptive predictive control of bioprocesses with constraint-based modeling and estimation. *Computers & Chemical Engineering* 135, 106744.
- Kager, J., Tuveri, A., Ulonska, S., Kroll, P., Herwig, C., 2020. Experimental verification and comparison of model predictive, PID and model inversion control in a *Penicillium chrysogenum* fed-batch process. *Process Biochemistry* 90, 1–11.
- Krausch, N., Kim, J., Barz, T., Lucia, S., Groß, S., Huber, M., Schiller, S., Neubauer, P., Cruz Bourmazou, M., 2022. High-throughput screening of optimal process conditions using model predictive control. *Biotechnology and Bioengineering* 119, 3584–3595.
- Lishkova, Y., Cannon, M., 2025. A successive convexification approach for robust receding horizon control. *IEEE Transactions on Automatic Control* URL: <https://arxiv.org/abs/2302.07744>.
- Lorenzen, M., Cannon, M., Allgöwer, F., 2019. Robust MPC with recursive model update. *Automatica* 103, 467–471.
- Lu, X., Cannon, M., 2023. Robust adaptive model predictive control with persistent excitation conditions. *Automatica* 152, 110959.
- Lu, X., Cannon, M., Koksál-Rivet, D., 2021. Robust adaptive model predictive control: Performance and parameter estimation. *International Journal of Robust and Nonlinear Control* 31, 8703–8724.
- Lucia, S., Engell, S., 2013. Robust nonlinear model predictive control of a batch bioreactor using multi-stage stochastic programming, in: European Control Conference (ECC), pp. 4124–4129.
- Mowbray, M., Petsagkourakis, P., Del Rio Chanona, E., Zhang, D., 2022. Safe chance constrained reinforcement learning for batch process control. *Computers and Chemical Engineering* 157, 107630.
- Rathore, A.S., Mishra, S., Nikita, S., Priyanka, P., 2021. Bioprocess control: Current progress and future perspectives. *Life* 11.
- Sankaranarayanan, P., Rengaswamy, R., 2022. CDiNN—convex difference neural networks. *Neurocomputing* 495, 153–168.
- Srinivasan, B., Bonvin, D., Visser, E., Palanki, S., 2003. Dynamic optimization of batch processes. *Computers and Chemical Engineering* 27, 27–44.
- Tuveri, A., Nakama, C.S., Matias, J., Holck, H.E., Jäschke, J., Insländ, L., Bar, N., 2023. A regularized moving horizon estimator for combined state and parameter estimation in a bioprocess experimental application. *Computers & Chemical Engineering* 172, 108183. doi:<https://doi.org/10.1016/j.compchemeng.2023.108183>.
- Yu, S., Maier, C., Chen, H., Allgöwer, F., 2013. Tube MPC scheme based on robust control invariant set with application to Lipschitz nonlinear systems. *Systems & Control Letters* 62, 194–200.